Opacity of neutral and low ion stages of Sn at the wavelength 13.5 nm used in extreme-ultraviolet lithography

M. Lysaght,[1] D. Kilbane,[2] N. Murphy,[1] A. Cummings,[1] P. Dunne,[1] and G. O'Sullivan[1]
[1]*Department of Physics, University College Dublin, Dublin 4, Ireland*
[2]*Center For Laser Plasma Research, Dublin City University, Glasnevin, Dublin 9, Ireland*
(Received 12 January 2005; published 15 July 2005)

Current research on sources for extreme ultraviolet lithography (EUVL) has converged on the use of discharge or laser produced plasmas containing xenon, tin, or lithium with tin showing by far the most promise. Because of their density, radiation transport from these plasmas is a major issue and accurate photoabsorption cross sections are required for the development of the plasma models needed to optimize conditions for source operation. The relative EUV photoionization cross sections of Sn I through Sn IV have been measured and from a comparison with the results of many body calculations, the cross section has been estimated to be close to 11 Mb in each species at 13.5 nm (91.8 eV), the wavelength of choice for EUVL.

DOI: 10.1103/PhysRevA.72.014502 PACS number(s): 32.30.Jc, 32.80.Fb

The wavelength of choice for extreme ultraviolet lithography (EUVL) has been selected as 13.5 nm, based on the availability of Mo/Si multilayer mirrors with reflectivity approaching 72% within a bandwidth of approximately 0.5 nm at this wavelength. A wide variety of sources based either on pulsed discharges or laser-produced plasmas (LPPs) are currently under investigation as potential sources. Most recent work has concentrated on three elements, Xe, Li, and Sn, as source materials. Xenon has the advantage that its inert gaseous nature can eliminate particulate debris, though the maximum conversion efficiency (CE) attained to date is approximately 0.8% for discharges [1] and 1.2% for LPPs [2]. The emission from a xenon plasma at 13.5 nm originates from $4p^64d^8 \rightarrow 4p^64d^75p$ transitions in a single ion stage, Xe^{10+} [3] and calculations based on steady state collisional-radiative model (CR), in which collisional ionization is balanced by three-body and radiative recombination [4], predict that the maximum attainable concentration of Xe^{10+} is only of the order of 40% [5]. More recently a CE value of 2% has been measured using the Lyman α line of Li III [6]. However emission from plasmas containing tin is potentially more intense than either [7] and CE values of up to 3% have already been reported [8] with a number of possible schemes for debris elimination proposed. These include the use of laser evaporated cavity confined tin vapor [9,10], mass limited tin doped droplets [11], liquid tin jets [12], and tin doped ceramics and glasses whose hardness limits the amount of particulate debris [13]. In the EUV spectrum of Sn, both atomic structure calculations and experiment demonstrate that the strongest lines result from $4p^64d^N \rightarrow 4p^54d^{N+1}+4p^64d^{N-1}4f$ $(1 \leqslant N \leqslant 6)$ transitions that form a line group near 13.5 nm [14]. Configuration interaction (CI) between the $4p^54d^{N+1}$ and $4p^64d^{N-1}4f$ configurations is known to be important and results in a spectral narrowing of the transition array [7,14]. More importantly, it is known that such transitions in adjacent ion stages, i.e., differing only in $4d$ subshell occupancy, tend to overlap in energy so that in the most extreme cases resonant emission from 10 ion stages can overlap in energy to yield an unresolved transition array (UTA) [15]. Such UTAs based on $4p^64d^N \rightarrow 4p^54d^{N+1}+4p^64d^{N-1}4f$ are the strongest features in EUV spectra [16] and derive their intensity from the transfer of oscillator strength from $4d \rightarrow \epsilon f$ photoionization resonances in the neutrals to $4d \rightarrow 4f$ transitions in the particular ions [17]. The emission within the required 2% bandwidth originates from Sn VIII through Sn XIII so in a 35–40 eV plasma, all ions present can contribute to the in-band emission resulting in theoretical CE values close to 5–6% [8,18]. The reason why this maximum CE has not been attained by experiment to date is that it is achieved in the plasma core and radiation trapping by low ion stages considerably reduces the observed intensity. In order to determine the maximum intensity that can be extracted it is necessary to have reliable information on the photoabsorption cross sections for the low ion stages of tin found in the plasma periphery. This letter directly addresses this problem and data are reported for the cross sections for neutral through four times ionized tin within the bandwidth of interest.

The dual laser plasma (DLP) technique in which the ions produced by one laser pulse are backlit by EUV continuum radiation from a second laser pulse was used to obtain the experimental data [19]. The spectra of Sn II through Sn IV were recorded photoelectrically with a 1024-element silicon photodiode array which was fiber-optically coupled to an image-intensified microchannel plate assembly, mounted on a 2.2 m grazing incidence vacuum spectrograph using a 1200 grooves/mm grating to give a photon energy resolution of $E/\Delta E$ of $\sim$1000. A 690 mJ, 15 ns Nd:YAG laser pulse was focused onto a pure tin target using a cylindrical lens to give a line plasma $\sim$12 mm in length while an 810 mJ, 15 ns Nd:YAG pulse tightly focused onto a tungsten target generated the backlighting continuum. The spectrum of Sn I was recorded under similar conditions using a Schwob–Fraenkel 2.2 m grazing incidence spectrometer at a spectral resolution, $\Delta\lambda \sim 0.42$ Å. By altering the interlaser time delay between the formation of the absorbing plasma column and the continuum emitting plasma, the laser irradiance on the absorbing target, or probing different plasma regions, it was possible to obtain absorption spectra dominated by a single ion stage. At an interlaser time delay of 500 ns and greater the absorption was mainly due to neutral tin, though it proved extremely difficult to obtain an appreciable population of this stage. At a delay of 300 ns the plasma was dominated by Sn II and at

a delay of 60 ns by Sn III and Sn IV ions which in fact proved difficult to isolate. Verification of the identity of the absorbing species was achieved by comparison with $4d \rightarrow 5p$ absorption from $4d^{10}5s^m5p^k$ ground configurations under identical experimental conditions [20–22].

In neutral tin the photoabsorption spectrum above the $4d$ threshold is dominated by a broad $4d \rightarrow \epsilon f$ resonance with discrete transitions which arise from $4d \rightarrow np$ excitation below threshold. Transitions of the type $4d \rightarrow nf$ are very weak because of the large centrifugal repulsion present in the $l = 3$ channel. With increasing ionization the centrifugal barrier disappears and $4f$ radial wave function contraction into the inner well region results in a transfer of oscillator strength from the continuum to the discrete spectrum [23–27]. The spectra of Sn I through Sn III are all dominated by a $4d \rightarrow \epsilon f$ continuum resonance and clearly show the intensity enhancement of discrete structure with increasing ionization. The discrete structure on the low energy side of the shape resonance, which corresponds to $4d \rightarrow nf$ transitions eventually becomes dominant at higher ion stages, though in the 13.5 nm region the continuum cross section remains essentially constant in the ion stages observed here.

To calculate the photoabsorption cross section the time dependent local density (TDLDA) approximation was used [28]. This approach has recently been shown to be very useful for studying changes in the $4d$ cross section with increasing ionization in iodine, cesium and antimony [29–31]. For these species the relativistic TDLDA code DAVID [32] was used to calculate the continuum cross section of each above the $4d$ threshold and compared with relative cross sections determined using the DLP technique. These calculations reproduced the cross section profile extremely well once the energies were shifted by a constant amount (1–10 eV) toward lower values. It is essential therefore to obtain experimental data to ascertain the energy shift. Radiation transport calculations performed to date have relied solely on theoretical input data. Use of *ab initio* TDLDA calculations would overestimate the cross section by a factor of ~ 2 because of the magnitude of the energy shift. Other approaches use single particle calculations with the Cowan suite of codes [34]. Such calculations greatly overestimate the cross section near threshold and would completely underestimate the absorption profile which is well above threshold in the present case [31].

Figure 1 demonstrates the evolution of the $4d$ absorption spectra from Sn I through Sn IV where $4f$ contraction causes a gradual enhancement of $4d \rightarrow 4f$ line intensities of the low energy side of the resonance with increasing ionization [Figs. 1(b) and 1(c)]. Also shown in Fig. 1(a) is the photoabsorption spectrum of Sn thin films recorded by Haensel *et al.* [35] which corresponds quite well with the present experimental results especially at low energies. The heights of the experimental spectra were scaled linearly in order to match them to the calculated TDLDA profiles and in addition a constant shift of 10 eV toward lower energies had to be applied to the calculated spectra to optimise agreement between theory and experiment. The same 10 eV shift to lower energies was required in the case of $4d \rightarrow \epsilon f$ resonance TDLDA calculations in antimony [30]. A shift of 7 eV to lower energies was again needed in the case of xenon in which spin-dependent

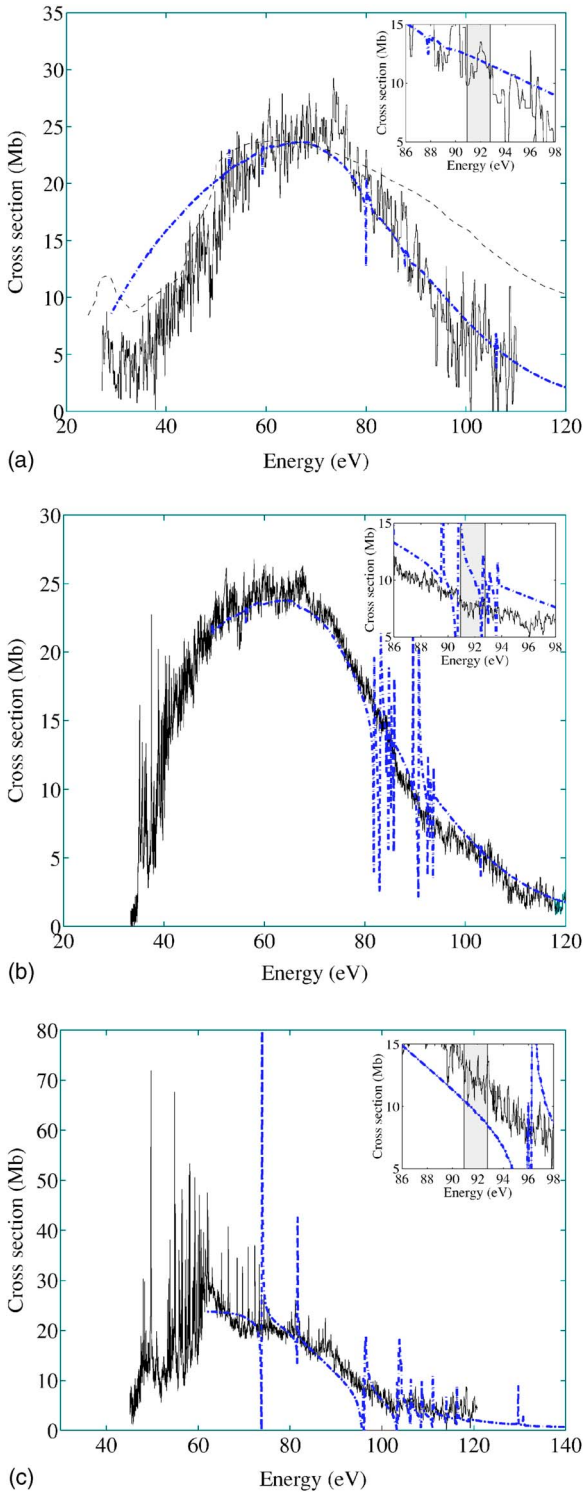

FIG. 1. (Color online). Comparison of experimental (solid, black) spectra recorded at time delays (a) $\Delta t = 500$, (b) 300, and (c) 60 ns with TDLDA calculations (dash-dot, blue) for the photoabsorption of Sn I, Sn II, and Sn IV. In the case of (c), the TDLDA calculations are shown for Sn IV as this stage appears to be slightly more dominant over Sn III upon analyzing the experimental spectrum. The shaded area in each of the insets is the required 2% bandwidth. Also included in (a) are the results of Haensel *et al.* (Ref. [35]) (dashed, black).

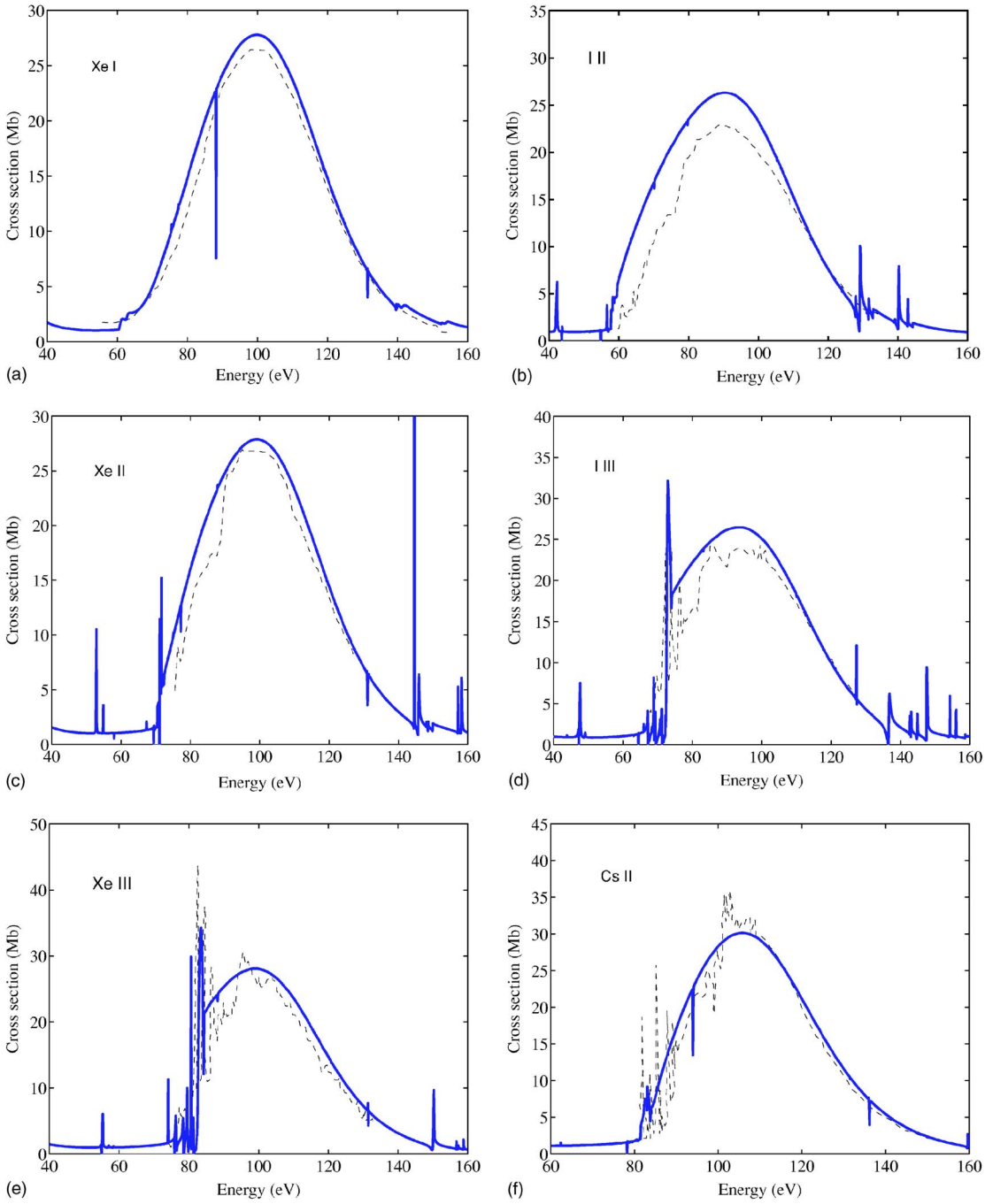

FIG. 2. (Color online). Comparison of experimental absolute photoionization cross sections for Xe I (Ref. [37]), Xe II–III (Ref. [38]), I II–III (Ref. [39]), and Cs II (Ref. [40]) (dashed, black) with TDLDA calculations (solid, blue) for the respective ion stages.

TDLDA calculations were performed [33]. This shift has its origin in the difference between the calculated and the experimental $4d$ binding energy. The agreement in overall profile above the $4d$ threshold, after this constant shift has been included, is seen to be good. The autoionization features due to nf contraction seen on the low energy side of the shape resonance in Figs. 1(b) and 1(c) are inadequately described by TDLDA calculations and are better accounted for using multiconfiguration Hartree Fock calculations. It should also be noted that the Fano-like profiles due to $p \rightarrow d,s$ excitations found on the high energy side of the shape resonance in Figs. 1(b) and 1(c) appear in relativistic TDLDA calculations for other elements also (Fig. 2) but are absent in both nonrelativistic TDLDA and RPAE calculations [36] and are not observed here.

Very little experimental data exist for absolute photoabsorption cross sections in this mid-Z region. Absolute measurements have been performed for Xe I–III [37,38], I II–III [39], and Cs II [40] using the merged beam technique. In order to justify the linear scaling of our experimental results to match theory, TDLDA calculated photoabsorption cross sections were compared with experimental data for the afor-

mentioned ion stages. Comparison of TDLDA results with experimental measurements showed agreement between theory and experiment to within 15% at the peak of the cross section. In Fig. 2 results from the relativistic TDLDA with experimental absolute cross sections were compared for ion stages of Xe [37,38], I [39], and Cs [40]. For the Xe spectra, a uniform shift in the theoretical results of 1.8 eV to lower energies was needed in order for the peak cross sections to match in Xe I–III. A shift of 4.5 and 1.5 eV to lower energies was needed for I II and I III, respectively, and for Cs II a shift of 1.5 eV to lower energies was required. It can be seen that in the case of Xe II, Xe III, I III, and Cs II that, although the TDLDA calculations are quite successful at giving a qualitative description of the $4d \rightarrow nf$ transitions found below the $4d$ threshold, quantitative agreement is less impressive and instead MCHF calculations better describe this behavior. This is most evident in the case of Cs II where it can be seen that although the autoionization resonances are quite clearly present in experiment, the TDLDA calculation does not predict them at all. Also, for the first and second ion stages of I and Xe the TDLDA predicts resonance structures in the high energy region above 130 eV which are clearly not present in the experimental data.

In addition, it should be observed that all of the measured cross sections for the above ion stages appear to be smaller than predicted from the TDLDA calculations especially at the peak cross section. This is most likely due to the neglect of relaxation effects which are known to be important in these spectra [38]. It can be seen that the largest discrepancy between theory and experiment occurs at the peak of each of the cross sections which in the case of xenon corresponds to a 5–10% difference. Relaxation effects for I II–III have been calculated by Ivanov [39] and have been shown to reduce random phase approximation values by 10–15%, leading to a very good agreement between theory and experiment. If this 10–15% reduction is applied to our iodine TDLDA calculations very good agreement is again obtained. It is interesting to observe that Itoh *et al.* [41] found that in the case of Xe II the difference between calculated results and experimental results is less on either side of the peak cross section which is again consistent with the results presented here. It is found that at 27 eV greater than the peak cross section the largest percentage difference of 9.0% occurred for Cs II. Since the cross section of interest for Sn I through IV is at 91.8 eV, which is $\approx$27 eV greater than the energy of the photoabsorption peak, a maximum error of $\pm 10\%$ is estimated. For Sn I and Sn II, calculations predict a cross section (σ) of 12 Mb at 13.5 nm and in the case of Sn III and Sn IV the calculations predict cross sections close to 10 Mb at this same wavelength. We would therefore expect that σ's $\approx 12 \pm 1.2$ and $\approx 10 \pm 1.0$ Mb, respectively, for these ions.

The authors would like to thank Dr. J. Costello and Dr. P. van Kampen of DCU. We also gratefully acknowledge Professor Indrek Martinson and Professor Ulf Litzén for making the Sn I measurements possible. This work was supported by Science Foundation Ireland (SFI) under Investigator Grant No. 02/IN.1/I99.

[1] N. R. Fornaciari *et al.*, Proc. SPIE **4688**, 110 (2002).
[2] H. Shields *et al.*, Proc. SPIE **4688**, 94 (2002).
[3] S. Churilov*et al.*, Opt. Lett. **28**, 1478 (2003).
[4] D. Colombant and G. F. Tonon, J. Appl. Phys. **44**, 3524 (1973).
[5] G. O'Sullivan *et al.*, Bull. Am. Phys. Soc. (to be published).
[6] D. Mayers *et al.*, *Third International EUVL Symposium, 2004*.
[7] G. O'Sullivan and R. Faulkner, Opt. Eng. **33**, 3978 (1994).
[8] K. Nishihara, *SPIE International Symposium Microlithography, 2004*.
[9] T. Aota and T. Tomie, Phys. Rev. Lett. **94**, 015004 (2005).
[10] T. Tomie *et al.*, Proc. SPIE **5037**, 147 (2003).
[11] M. Richardson *et al.*, Proc. SPIE **5196**, 119 (2004).
[12] P. A. C. Jansson *et al.*, Appl. Phys. Lett. **84**, 2256 (2004).
[13] G. O'Sullivan *et al.*, Proc. SPIE **5196**, 273 (2004).
[14] P. Mandelbaum *et al.*, Phys. Rev. A **35**, 5051 (1987).
[15] D. O'Reilly *et al.*, Appl. Phys. Lett. **76**, 34 (2000).
[16] G. O'Sullivan and P. K. Carroll, J. Opt. Soc. Am. **71**, 227 (1982).
[17] G. O'Sullivan, in *Giant Resonances in Atoms, Molecules and Solids*, edited by J. P. Connerade, J. M. Esteva, and R. C. Karnatak (Plenum, New York, 1987).
[18] A. Cummings *et al.*, J. Phys. D **38** (4), 604-616 (2005).
[19] J. T. Costello *et al.*, Phys. Scr., T **34**, 77 (1991).
[20] J. P. Connerade and M. A. P. Martin, Proc. R. Soc. London, Ser. A **357**, 103 (1977).
[21] P. Dunne *et al.*, J. Phys. B **32**, L597 (1999).
[22] G. Duffy *et al.*, J. Phys. B **34**, 3171 (2001).
[23] R. I. Karaziya, Sov. Phys. Usp. **24**, 775 (1981).
[24] K. Nuroh *et al.*, Phys. Rev. Lett. **49**, 862 (1982).
[25] G. O'Sullivan, J. Phys. B **15**, L765 (1982).
[26] K. T. Cheng and C. Froese Fischer, Phys. Rev. A **28**, 2811 (1983)
[27] S. Kucas *et al.*, Lith. J. Phys. **23**, 34 (1983) [Sov. Phys. Collect. **28**, 36 (1983)].
[28] A. Zangwill and P. Soven, Phys. Rev. A **21**, 1561 (1980).
[29] G. O'Sullivan, *et al.*, Phys. Rev. A **53**, 3211 (1996).
[30] R. D'Arcy *et al.*, J. Phys. B **33**, 1383 (2000).
[31] A. Cummings *et al.*, Phys. Rev. A **63**, 022702 (2001).
[32] A. Zangwill and D. A. Liberman, Comput. Phys. Commun. **32**, 75, (1984).
[33] X.-M. Tong *et al.*, J. Phys. B **33**, 717 (2000).
[34] R. D. Cowan, *The Theory of Atomic Structure and Spectra* (University of California Press, Berkeley, 1981).
[35] R. Haensel *et al.*, Appl. Opt. **7**(2), 301-306 (1968).
[36] G. Gribakin (private communication).
[37] J. B. West and J. Morton, At. Data Nucl. Data Tables **22**, 103 (1978).
[38] P. Andersen *et al.*, J. Phys. B **34**, 2009 (2001).
[39] H. Kjeldsen *et al.*, Phys. Rev. A **62**, 020702(R) (2000).
[40] H. Kjeldsen *et al.*, J. Phys. B **35**, 2845 (2002).
[41] Y. Itoh *et al.*, J. Phys. B **34**, 3493 (2001).